

9,10-Anthracene dicarboxylate bridged complexes with M_2 quadruply bonded dimetal units: $[\{M_2(O_2C^tBu)_3\}_2(\mu-9,10-An(CO_2)_2)]$, where $M = Mo$ or W

Matthew J. Byrnes,^a Malcolm H. Chisholm,^{*,a} David F. Dye,^a Christopher M. Hadad,^{*,a} Brian D. Pate,^a Paul J. Wilson^{†,b} and Jeffrey M. Zaleski^{*,a}

^a Department of Chemistry, The Ohio State University, 100 W. 18th Avenue, Columbus, OH, 43210-1185, USA.

E-mail: chisholm@chemistry.ohio-state.edu; hadad@chemistry.ohio-state.edu; zaleski@indiana.edu.

^b Department of Chemistry, Indiana University, 800 East Kirkwood Avenue, Bloomington, Indiana 47405, USA. E-mail: chisholm@chemistry.ohio-state.edu

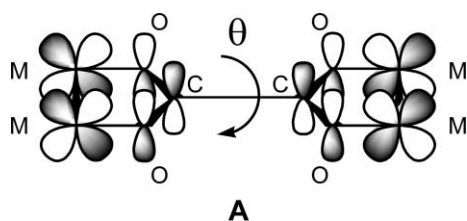
Received 9th October 2003, Accepted 1st December 2003

First published as an Advance Article on the web 12th January 2004

From the reactions between $[M_2(O_2C^tBu)_4]$ and 9,10-anthracenedicarboxylic acid in toluene, the dicarboxylate bridged complexes $[\{M_2(O_2C^tBu)_3\}_2(\mu-9,10-An(CO_2)_2)]$, have been obtained as microcrystalline yellow ($M = Mo$) and red ($M = W$) powders. The powders are soluble in THF forming intense red ($M = Mo$) and green ($M = W$) solutions. The electronic absorption spectra in 2-MeTHF have been recorded as a function of temperature (2–298 K) and show a small bathochromic shift on cooling. The electronic structures have been investigated by molecular orbital calculations employing density functional theory on the model compounds $[(HCO_2)_3M_2]_2(\mu-9,10-An(CO_2)_2)$ where the M_4 unit is constrained to lie in a plane. These reveal a minimum energy, gas-phase structure wherein the plane of the anthracene is twisted by *ca.* 54° with respect to its 9,10-carboxylate units for both Mo and W. The results of these calculations are correlated with the electronic absorption spectral data and the electrochemical measurements (CV and DPV) of the first and second oxidation waves. The EPR spectra of the radical cations formed by single-electron oxidation with $[Cp_2Fe]^+[PF_6]^-$ in a THF-CH₂Cl₂ solvent mixture show that the complexes are valence trapped at ambient temperature on the EPR timescale. These results are discussed in the light of recent studies of dicarboxylate-linked MM quadruple bonds.

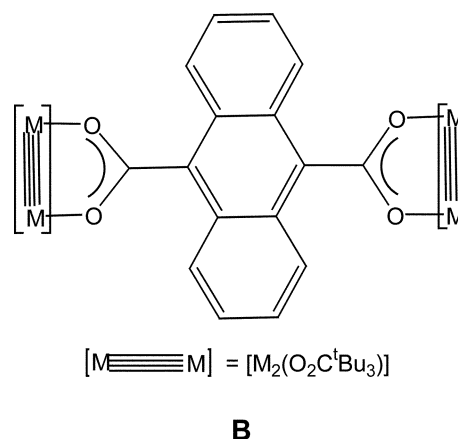
Introduction

When two MM quadruply bonded complexes are united by a dicarboxylate ligand electronic coupling arises as a result of $M_2 \delta$ to bridge π -conjugation.^{1–3} For a given $O_2C-X-CO_2$ bridge, the CO_2 units are both the alligator clips and the switch because the coupling between the two dinuclear centers is dependent on the dihedral angle θ between the two CO_2 planes as exemplified by the simple case of the oxalate bridge shown below in A.⁴



When $\theta = 0^\circ$ (D_{2h} symmetry), the coupling is at a maximum, and when $\theta = 90^\circ$ (D_{2d} symmetry), the coupling is at a minimum. As we have described in some detail for the cases of oxalate and perfluoroterephthalate bridged MM quadruply bonded complexes, this situation leads to marked thermochromism in solution and in frozen glasses because thermal energy is comparable to the barriers of rotation about the C–C bonds (oxalate or carboxylate-phenyl).^{4,5} According to the electronic structure calculations, the planar D_{2h} geometry ($\theta = 0^\circ$) is favored over the twisted geometry ($\theta = 90^\circ$) by 5–8 kcal mol⁻¹ for oxalate⁴ and 2–5 kcal mol⁻¹ for perfluoroterephthalate bridges where the lower and higher numbers refer to the complexes where $M = Mo$ and W , respectively.⁵ Upon cooling from room temper-

ature to 80 K or lower, the lowest energy transition shifts to longer wavelengths by 50 nm for oxalate and well over 100 nm for perfluoroterephthalate.^{4,5} We describe here our studies of 9,10-anthracene dicarboxylate bridged M_2 quadruply bonded compounds of molybdenum and tungsten shown in B. The mutual competition between extended π -conjugation and steric factors is well known for 9,10-disubstituted anthracene complexes, *e.g.* 9,10- $R_2-C_{14}H_8$ where R is an ester,⁶ ketone^{7,8} or imine.^{7,9} As we show here this bridge has interesting consequences in linking MM quadruple bonds.



Results and discussion

Synthesis

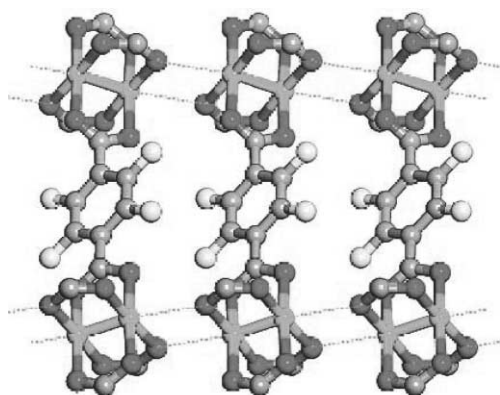
The bridged complexes $[\{M_2(O_2C^tBu)_3\}_2(\mu-9,10-An(CO_2)_2)]$ ($M = Mo, W$; 9,10- $An(CO_2)_2 = 9,10$ -anthracenedicarboxylate) precipitated as intensely colored solids ($Mo = yellow$; $W = red$)

[†] Present Address: Department of Chemistry, University of Bath, Bath, UK BA2 7AY.

from toluene after stirring 2 equivalents of $[M_2(O_2C^iBu)_4]$ with 9,10-An(CO₂H)₂ for 7–10 days. These bridged complexes form intense red (M = Mo) and green (M = W) colored solutions when dissolved in THF (see below). Both compounds are pure as determined by ¹H NMR spectroscopy in d₈-THF. The elemental analysis of the tungsten compound was a little low in carbon, a result which has been seen before in the analysis of similar compounds.^{10,11}

Molecular and electronic structures

We have not determined the solid-state molecular structures of these 9,10-anthracenedicarboxylate complexes by single-crystal X-ray diffraction studies but propose that in the solid state, they adopt coordination polymeric structures similar to that deduced for the μ -O₂CC₆F₄CO₂ bridged complexes from powder X-ray diffraction data.⁵ In this way, each M₂ unit associates with its nearest intermolecular neighbors by way of weak M₂ ··· O bonds and the C₆F₄ ring, and in this case the anthracene, loses conjugation with the M₂O₂C units as shown in C.



C

In order to interrogate the electronic structure of these anthracenedicarboxylate bridged complexes, we have undertaken molecular orbital calculations employing density functional theory on the model formate compounds $[M_2(O_2CH)_3]_2(\mu$ -9,10-An(CO₂)₂) using the Gaussian 98 programs,¹² employing the B3LYP^{13–15} functional in conjunction with the 6-31G* (SD) basis set for H, C and O,¹⁶ and the SDD energy consistent pseudo-potentials for Mo and W.¹⁷ To further simplify this approach, we constrained the two M₂ centers and their attendant ligands to undergo correlated motions about the anthracene plane such that D₂ symmetry was always maintained. This approach was previously taken for the perfluoroterephthalate-linked M₂ complexes.⁵ The calculations were initially performed under D₂ symmetry with a starting dihedral angle of 45° between the anthracene ring and the two M₂ units plane, and both converged on ~54°. These minima were then tested by starting the calculations near 0°, where the anthracene lies in the pseudo M₄ plane, and near 90° in turn, also under D₂ symmetry. In each case, the structure returned to the minimum energy at ~54°. The limiting D₂ structures were calculated under rigorous D_{2h} symmetry corresponding to $\theta = 0^\circ$ and 90°.

The all-planar D_{2h} structure, $\theta = 0^\circ$, that allows maximum M₂ δ to bridge π -conjugation, is not favored on steric grounds because of the unfavorable *peri*-CH to O interactions involving the protons at the 1, 4, 5 and 8 positions. These D_{2h} structures ($\theta = 0^\circ$) are calculated to be higher in energy by 12.8 (M = Mo) and 11.7 kcal mol⁻¹ (M = W) relative to the minimum energy twisted structure with D₂ symmetry where $\theta = \sim 54^\circ$. The D_{2h} structures in which the anthracene ring is perpendicular to the M₄ plane ($\theta = 90^\circ$) are higher in energy by 1.3 (M = Mo) and 1.7 kcal mol⁻¹ (M = W) relative to the twisted ($\theta = \sim 54^\circ$) structures.

Taking these three structures as limiting energy conformations, one can see that rotation about the carboxylate carbon O₂C–C_{ipso} bonds will be possible at room temperature, but at low temperatures, the preferred motion will be an oscillation about the $\theta = 90^\circ$ structure with a double minimum potential well at $\theta = 54$ and 126° as shown in Fig. 1. In reality, the molecular motions of the molecule will not be correlated and D₂-symmetry will not be maintained. However, it is not practical to perform calculations with completely unrestricted rotational constraints. Nevertheless, it is reasonable to assume that the D₂ structure with $\theta = 54^\circ$ represents a minimum energy structure (Fig. 2), it should be noted that when either [M₂(O₂C)₄] unit is orthogonal to the anthracene plane, coupling to the other M₂ unit is lost.

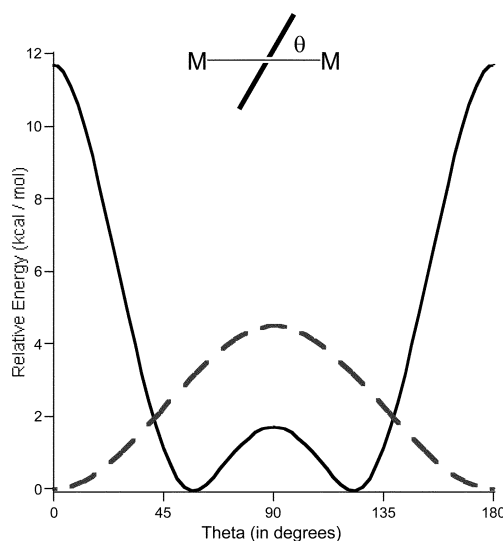


Fig. 1 Calculated energy maxima for $[W_2(O_2CH)_3]_2(\mu$ -O₂C-1,4-C₆F₄CO₂) (---) and $[W_2(O_2CH)_3]_2(\mu$ -9,10-An(CO₂)₂) (—) as a function of θ .

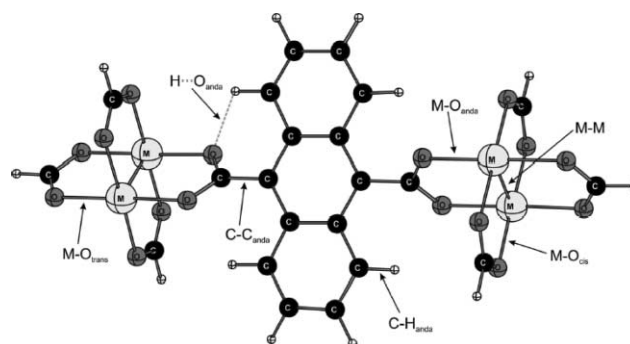


Fig. 2 View of the twisted D₂ ($\theta = \sim 54^\circ$) calculated formate structure $[M_2(O_2CH)_3]_2(\mu$ -9,10-An(CO₂)₂) (where M = Mo, W). Corresponding selected geometrical data are given in Table 1.

The optimized geometries for the three cases considered in this work are summarized in Table 1. The orbital energies of the frontier orbitals, the two δ combinations, the HOMO and the HOMO – 1, the LUMO, LUMO + 1 and LUMO + 2 are given in Table 2 and are shown in Fig. 3. The calculated energies of the M₂ δ to bridge π^* charge transfer transition, based on time dependent DFT calculations^{18–22} are given in Table 3.

In the two D_{2h} structures, $\theta = 0$ and 90°, the M₂ δ combinations transform as b_{2g} and b_{3u}. With the anthracene in the plane of the M₄ unit, the b_{3u} combination has a symmetry match to allow back-bonding to the LUMO of the O₂CAnCO₂ bridge. This results in a splitting of the HOMO, the b_{2g} molecular orbital, and the HOMO – 1, b_{3u}, by ca. 0.4 eV for M = W. When $\theta = 90^\circ$, these two M₂ δ combinations are isoenergetic and in rigorous D_{2h} symmetry degenerate. With $\theta = \sim 54^\circ$, the mole-

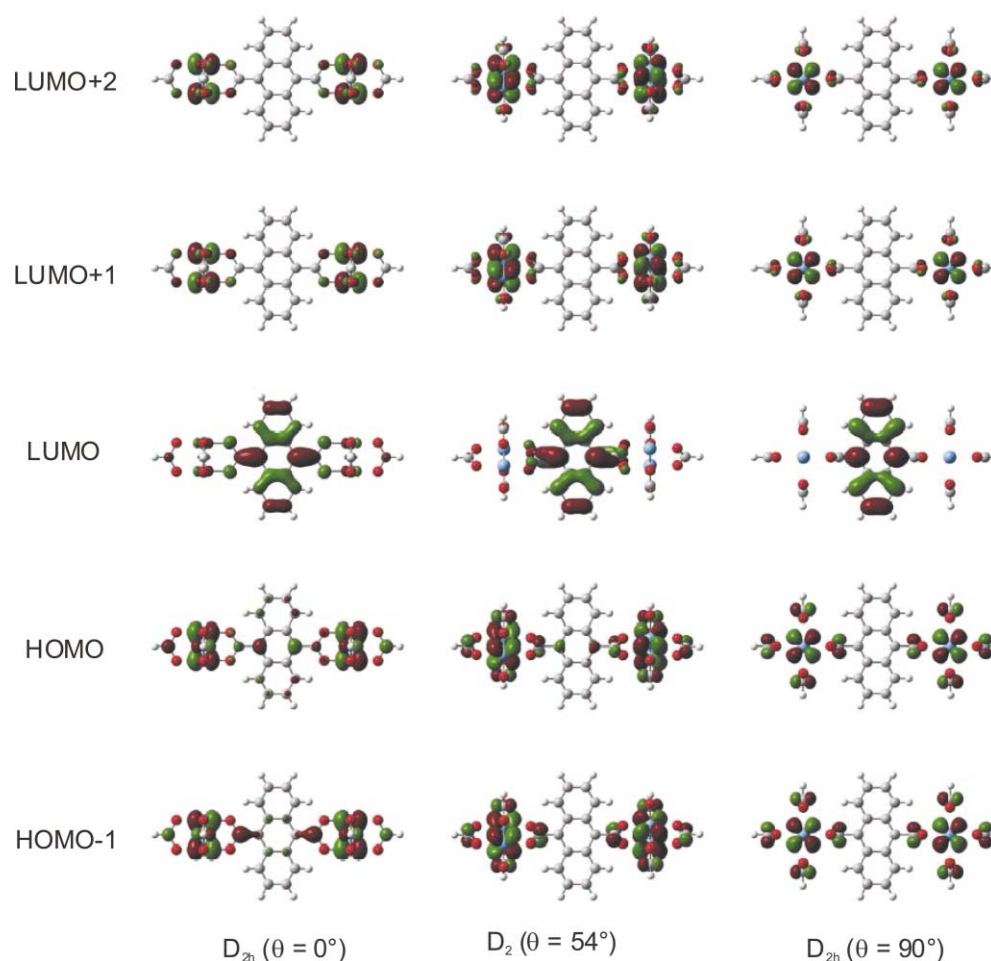


Fig. 3 GaussView representations of the frontier molecular orbitals of D_{2h} ($\theta = 0^\circ$), D_2 ($\theta = \sim 54^\circ$) and D_{2h} ($\theta = 90^\circ$) [$\{W_2(O_2CH)_3\}_2(\mu-9,10-An(CO_2)_2)$].

Table 1 Calculated geometric data for the D_{2h} ($\theta = 0^\circ$), D_2 ($\theta = \sim 54^\circ$) and D_{2h} ($\theta = 90^\circ$) conformations of the formate models [$\{M_2(O_2CH)_3\}_2(\mu-9,10-An(CO_2)_2)$] ($M = Mo, W$)

	Mo D_{2h} ($\theta = 0^\circ$)	Mo D_2 ($\theta = \sim 54^\circ$)	Mo D_{2h} ($\theta = 90^\circ$)	W D_{2h} ($\theta = 0^\circ$)	W D_2 ($\theta = \sim 54^\circ$)	W D_{2h} ($\theta = 90^\circ$)
M–M	2.116	2.118	2.118	2.199	2.203	2.201
M–O _{anda}	2.085	2.105	2.113	2.066	2.092	2.104
M–O _{trans}	2.127	2.123	2.123	2.121	2.113	2.113
M–O _{cis}	2.122	2.123	2.124	2.112	2.109	2.112
C–C _{anda}	1.507	1.492	1.499	1.494	1.488	1.497
C–H _{anda}	1.072	1.082	1.085	1.071	1.082	1.085
H ··· O _{anda}	1.888	2.333	2.928	1.888	2.330	2.930

Table 2 Comparison of the frontier molecular orbital energies of D_{2h} ($\theta = 0^\circ$), D_2 ($\theta = \sim 54^\circ$) and D_{2h} ($\theta = 90^\circ$) [$\{M_2(O_2CH)_3\}_2(\mu-9,10-An(CO_2)_2)$] ($M = Mo, W$) molecules.

	Mo D_{2h} ($\theta = 0^\circ$)	Mo D_2 ($\theta = 54^\circ$)	Mo D_{2h} ($\theta = 90^\circ$)	W D_{2h} ($\theta = 0^\circ$)	W D_2 ($\theta = 54^\circ$)	W D_{2h} ($\theta = 90^\circ$)
LUMO + 2	A _u (–2.127)	A (–2.152)	A _u (–2.170)	A _u (–1.354)	A (–1.352)	B _{1g} (–1.358)
LUMO + 1	B _{1g} (–2.129)	B ₁ (–2.152)	B ₁ (–2.170)	B _{1g} (–1.356)	B ₁ (–1.352)	A _u (–1.359)
LUMO	B _{3u} (–2.882)	B ₃ (–2.366)	B _{2u} (–2.201)	B _{3u} (–2.804)	B ₃ (–2.334)	B _{2u} (–2.175)
HOMO	B _{2g} (–5.175)	B ₂ (–5.322)	B _{2g} (–5.467)	B _{2g} (–4.668)	B ₂ (–4.815)	B _{2g} (–4.913)
HOMO – 1	B _{3u} (–5.510)	B ₃ (–5.470)	B _{3u} (–5.470)	B _{3u} (–5.053)	B ₃ (–4.941)	B _{3u} (–4.916)

cule has D_2 symmetry and the M_2 δ combinations transform as b_2 and b_3 . The combination of b_3 symmetry still allows some back-bonding to the anthracenedicarboxylate, but the resulting splitting of the HOMO and HOMO – 1 molecular orbitals, b_2 and b_3 , is smaller at *ca.* 0.15 eV relative to the all-planar D_{2h} $\theta = 0^\circ$ structure. In each geometry, the LUMO is a bridge-based, π -molecular orbital. At $\theta = 90^\circ$, this does not mix with the two 9,10-CO₂ moieties but at $\theta = 0^\circ$, there is extensive CO₂ involvement. Consequently, the LUMO, the b_{3u} orbital, in D_{2h} symmetry varies by *ca.* 0.6 eV as a function of θ , and the HOMO to

LUMO electronic transition is expected to vary accordingly. As seen from an inspection of Table 3, the HOMO–LUMO energy gap, the predicted excitation wavelength and perhaps even more significantly, the oscillator strength (intensity), which correlates with the M_2 δ to bridge overlap, are very sensitive to θ .

For the minimum energy structures with $\theta = \sim 54^\circ$, the HOMO – 2 is for both $M = Mo$ and W a 9,10-An(CO₂)₂ π orbital at *ca.* –5.7 eV. In the case of tungsten, there are four molecular orbitals which are close in energy at *ca.* –6.3 eV corresponding to the M_2 π combinations. Below these orbitals,

Table 3 Calculated lowest $M_2 \delta$ to 9,10-An(CO₂)₂ π^* transition energies determined by TDDFT for the formate models of [$\{M_2(O_2CH)_3\}_2(\mu-9,10-An(CO_2)_2)$] ($M = Mo, W$).

	λ_{max} (Calc.)/nm	λ_{max} (Calc.)/eV	Calculated oscillator strength (f)
Mo D_{2h} ($\theta = 0^\circ$)	618	2.01	0.628
Mo D_2 ($\theta = \sim 54^\circ$)	496	2.50	0.254
Mo D_{2h} ($\theta = 90^\circ$)	443	2.80	0.000
W D_{2h} ($\theta = 0^\circ$)	726	1.71	0.823
W D_2 ($\theta = \sim 54^\circ$)	603	2.06	0.303
W D_{2h} ($\theta = 90^\circ$)	558	2.22	0.000

in the range -6.8 to -7.3 eV, are two anthracene based π -molecular orbitals and the two $M_2 \sigma$ molecular orbitals. In the case of molybdenum, the $M_2 \pi$ and anthracene π molecular orbitals are close in energy at *ca.* -7.2 eV.

It is worth noting here that electronic structure calculations on the free 9,10-anthracenedicarboxylic acid predict a ground state structure with C_1 symmetry and a θ angle of $\sim 50^\circ$ with a HOMO–LUMO energy gap of ~ 3.3 eV. This structure closely resembles that found in the solid state for 9,10-anthracenedicarboxylate dimethyl ester.⁶ For certain bulky substituents such as ketones and imines, the dihedral angle has been observed to be of the order of 75° , and experimental barriers to rotations as high as 26 kcal mol⁻¹ have been determined.⁷

Electronic absorption spectra

In the solid-state, the molybdenum complex is yellow and the tungsten complex is red. The electronic absorption spectra recorded as Nujol mulls at 298 K are shown in Fig. 4. In the case of tungsten, the anthracene based π – π^* transition at 370 nm, which shows some evidence of a vibronic progression, is well separated from the longer wavelength absorption centered at 557 nm. The latter we assign to the metal to bridge π^* transition of a low symmetry M_4 bridged molecule that does not enjoy extensive M_2 –bridge– M_2 conjugation. In the case of molybdenum, this transition occurs close in energy to the anthracene π – π^* transition at 420 nm.

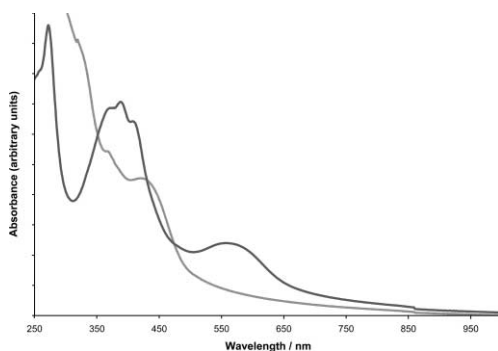


Fig. 4 Electronic absorption spectra of [$\{M_2(O_2C^tBu)_3\}_2(\mu-9,10-An(CO_2)_2)$] ($M = Mo$ (grey line), W (black line)) as a Nujol mull at room temperature (There is a grating change at *ca.* 860 nm).

The room-temperature spectra of the molybdenum and tungsten complexes dissolved in THF, along with that of the free dicarboxylic acid, are compared in Fig. 5. Band maxima and molar absorptivities for the free acid as well as both dimetal complexes are given in Table 4 along with several other dimolybdenum and ditungsten bridged complexes. The free acid and the molybdenum complex show great similarity in the region 400–350 nm region where the anthracene π – π^* transition shows an extensive vibronic progression. The molybdenum complex shows an additional lower energy (longer wavelength) absorption centered at 497 nm which is assignable to the $M_2 \delta$ to bridge charge transfer transition. At higher energy (shorter wavelength), the molybdenum complex shows a broad absorption centered at 300 nm. This is common to [$M_2(O_2CR)_4$] compounds and, in this instance, can be assigned to $M_2 \delta$ to

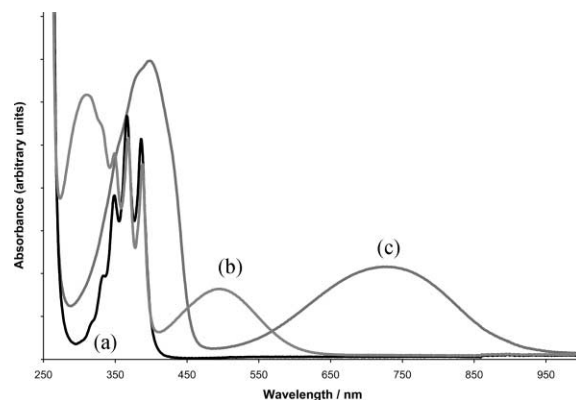


Fig. 5 Electronic absorption spectra of 9,10-An(CO₂H)₂ (a) and [$\{M_2(O_2C^tBu)_3\}_2(\mu-9,10-An(CO_2)_2)$] ($M = Mo$ (b), W (c)) in THF at room temperature (There is a grating change at *ca.* 860 nm).

$CO_2 \pi^*$ transitions associated with the pivalate ligands. The spectrum of the tungsten complex shows an intense absorption from 350–450 nm which we assign to an overlap of the $W_2 \delta$ to CO_2 (pivalate) π^* and anthracene π – π^* transitions. Of major significance is the broad intense absorption centered at 728 nm. This is assigned to the $M_2 \delta$ to bridge π^* transitions which for tungsten is moved to lower energy and enjoys a higher molar absorptivity relative to its molybdenum analogue. The red-shift of the $M_2 \delta$ to $CO_2 \pi^*$ and bridge π^* transition for $M = W$ relative to $M = Mo$ is consistent with previous related studies^{4,5,10,11} and correlates well with the relative energies of the $M_2 \delta$ orbitals.²³ The difference between the solid-state electronic absorption spectra and those in solution is quite dramatic when Figs. 4 and 5 are compared. The tungsten complex is a “stop and go” complex being red in the solid-state and green in solution.

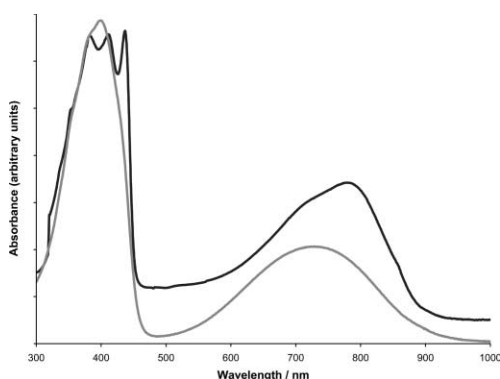
In contrast to the spectra of perfluoroterephthalate bridge complexes,⁵ the electronic absorption spectra show little temperature dependence. The electronic absorption spectra of the tungsten complex recorded at room temperature in THF is compared with that recorded at 10 K in a 2-MeTHF glass in Fig. 6. There is no detectable change in the spectra measured between 2–10 K. At 2 K, the $M_2 \delta$ to bridge π^* transition is shifted *ca.* 60 nm to longer wavelength relative to the room temperature spectrum and shows some evidence of the emergence of a vibronic progression. The changes in the electronic absorption spectra of the perfluoroterephthalate bridged tungsten complex are much more dramatic on cooling.⁵ We propose that these differences can be correlated with the energy minima profile as a function of θ for the two complexes as shown in Fig. 1.

Electrochemical studies

We have examined, by cyclic voltammetry (CV) and differential pulse voltammetry (DPV), the redox properties of the molybdenum and tungsten complexes in THF with a silver wire pseudo-reference electrode. Both compounds show evidence of two closely separated one-electron oxidations. For molybdenum, the first oxidation occurs close to that of ferrocene, while the tungsten complex is more easily oxidized by roughly

Table 4 Electronic absorption data for the various dicarboxylate complexes

Compound	λ_{\max}/nm (THF)	E/eV (THF)	$\epsilon/M^{-1} \text{ cm}^{-1}$ (THF)
9,10-An(CO ₂ H) ₂	386	3.038	5 500
	366	3.204	5 900
	349	3.360	4 200
	333	3.522	2 100
4 [Mo ₂ (O ₂ C ^t Bu) ₃] ₂ (μ -9,10-An(CO ₂) ₂)	497	2.360	4 200
	388	3.023	12 100
	368	3.187	13 700
	349	3.360	12 700
	311	3.771	16 500
	[W ₂ (O ₂ C ^t Bu) ₃] ₂ (μ -9,10-An(CO ₂) ₂)	728 399	1.611 2.939
[Mo ₂ (O ₂ C ^t Bu) ₃] ₂ (μ -1,8-An(CO ₂) ₂) ^a	504	2.327	10 100
	394 sh	2.977	8 400
	370 sh	3.170	12 200
	358	3.276	14 200
	320 sh	3.665	16 400
	286	4.101	21 500
	[W ₂ (O ₂ C ^t Bu) ₃] ₂ (μ -1,8-An(CO ₂) ₂) ^a	716 470 368 348 sh	1.638 2.495 3.187 3.370
[Mo ₂ (O ₂ C ^t Bu) ₃] ₂ (μ -1,4-C ₆ F ₄ (CO ₂) ₂) ^a	470	2.495	10 500
	322 sh	3.642	11 900
	288	4.072	18 000
[W ₂ (O ₂ C ^t Bu) ₃] ₂ (μ -1,4-C ₆ F ₄ (CO ₂) ₂) ^a	816	1.437	27 000
	354	3.313	17 300

^a Taken from ref 11.**Fig. 6** Electronic absorption spectra of [W₂(O₂C^tBu)₃]₂(μ -9,10-An(CO₂)₂) in THF at room temperature (grey line) and in a 2-MeTHF glass at 10 K (black line) (There is a grating change at *ca.* 860 nm).

half a volt. This oxidation behavior is similar to that previously reported for other dicarboxylate bridged compounds of molybdenum and tungsten, and a pertinent comparison is given in Table 5. The DPV for the tungsten complex is shown in Fig. 7. Quite notable here is the relatively small $\Delta E_{1/2}$ between the first and second waves, particularly when compared to oxalate and perfluoroterephthalate.¹¹ Even the 1,8-anthracenedicarboxylate bridge serves more effectively to couple the two dimetal centers.¹¹ Qualitatively, this correlates well with the relatively small calculated energy difference between the two M₂ δ combinations *ca.* 0.1–0.15 eV, for $\theta \sim 54^\circ$. It should be noted that the $\Delta E_{1/2}$ obtained for [W₂(O₂C^tBu)₃]₂(μ -9,10-An(CO₂)₂) is comparable to that reported for [W₂(O₂C^tBu)₃]₂(μ -1,1'-Fe(η^5 -C₅H₄(CO₂)₂)).¹¹ Both [M₂(O₂C^tBu)₃]₂(μ -9,10-An(CO₂)₂) (M = Mo, W) complexes also show two quasi-reversible reduction waves at *ca.* -2.1 V and -2.3 to -2.5 V (*vs.* Cp₂Fe^{0/+}) which probably correspond to the reduction of the anthracene bridge based upon the calculated values for the LUMO reported in

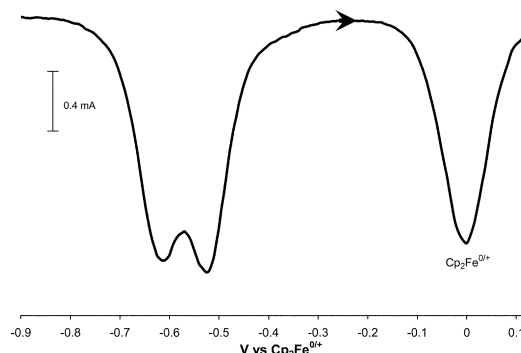
**Fig. 7** Differential pulse voltammetry (DPV) of [W₂(O₂C^tBu)₃]₂(μ -9,10-An(CO₂)₂) in 0.5 M ⁿBu₄NPF₆ / THF showing the two oxidation processes relative to ferrocene. Scan rate = 20 mV s⁻¹.

Table 2. They are not likely to be metal-based reductions. The properties of these reduction processes have not been investigated further.

EPR of the one-electron oxidized radical cations

As a further test of the electronic communication between the M₂ centers, we have oxidized the compounds in reactions with [Cp₂Fe]⁺[PF₆]⁻ and examined the EPR spectra of the resultant solutions in a THF-CH₂Cl₂ solvent mixture. The EPR spectra of the molybdenum complex are temperature independent and can be assigned to a valence trapped radical cation where one dinuclear center is present as Mo₂⁵⁺ with a valence MO bonding description of MM $\sigma^2\pi^4\delta^1$. Specifically, the *g* and *A* values arising from coupling to ⁹⁵Mo and ⁹⁷Mo (both *I* = 5/2, 25% combined natural abundance) are essentially identical to that seen for the [Mo₂(O₂C^tBu)₄]⁺ radical cation.²⁴ A similar situation was observed for the oxidized radical cation [Mo₂(O₂C^tBu)₃]₂(μ -O₂CC₆F₄CO₂)⁺[PF₆]⁻.²⁴ We would like to emphasize that from inspection of Table 5 neither

Table 5 Comparison of electrochemical oxidation potentials^a for various linked and unlinked MM quadruply bonded complexes with pivalate ligands referenced to [Cp₂Fe]^{0/+}

Compound	$E_{1/2}^1/V$	$E_{1/2}^2/V$	$\Delta E_{1/2}/mV$
[{Mo ₂ (O ₂ C ^t Bu) ₃ } ₂ (μ-9,10-An(CO ₂) ₂)]	+0.04	+0.10	60
[{W ₂ (O ₂ C ^t Bu) ₃ } ₂ (μ-9,10-An(CO ₂) ₂)]	-0.62	-0.53	90
[{Mo ₂ (O ₂ C ^t Bu) ₃ } ₂ (μ-C ₂ O ₄)] ^b	-0.03	+0.25	280
[{W ₂ (O ₂ C ^t Bu) ₃ } ₂ (μ-C ₂ O ₄)] ^b	-1.26	-0.54	717
[{Mo ₂ (O ₂ C ^t Bu) ₃ } ₂ (μ-1,4-C ₆ F ₄ (CO ₂) ₂)] ^b	+0.10		65
[{W ₂ (O ₂ C ^t Bu) ₃ } ₂ (μ-1,4-C ₆ F ₄ (CO ₂) ₂)] ^b	-0.66	-0.37	285
[{W ₂ (O ₂ C ^t Bu) ₃ } ₂ (μ-1,8-An(CO ₂) ₂)] ^b	-0.66	-0.51	156
[{W ₂ (O ₂ C ^t Bu) ₃ } ₂ (μ-1,1'-Fe(η ⁵ -C ₅ H ₄ CO ₂) ₂)] ^b	-0.81	-0.72	93
[Mo ₂ (O ₂ C ^t Bu) ₄] ^b	-0.04		
[W ₂ (O ₂ C ^t Bu) ₄] ^b	-0.70		

^a $E_{1/2}^1$ and $E_{1/2}^2$ values correspond to E_p^1 and E_p^2 , respectively. No attempt has been made to convert E_p to $E_{1/2}$ according to the methodology of Richardson and Taube.³⁰ ^b Taken from ref. 11.

[{Mo₂(O₂C^tBu)₃}₂(μ-9,10-An(CO₂)₂)] nor [{Mo₂(O₂C^tBu)₃}₂(μ-1,4-C₆F₄(CO₂)₂)] would be expected to be oxidized by [Cp₂Fe]⁺[PF₆]⁻ in THF. However, it has been reported that the oxidation potential of [Cp₂Fe] is 100 mV higher in CH₂Cl₂ than in THF²⁵ and this presumably accounts for the generation of the dimolybdenum radical cations in the mixed solvent system.

The spectra obtained upon oxidation of the tungsten complex were more complex. At 240 K and above, the signal was rather broad but otherwise similar to [W₂(O₂C^tBu)₄]⁺ and assignable to a valence trapped W₂⁵⁺ center having $g = 1.83$, $A = 60$ G due to ¹⁸³W, $I = 1/2$ (14% natural abundance). These parameters are essentially identical to those for [W₂(O₂C^tBu)₄]⁺[PF₆]⁻.²⁴ However, upon lowering the temperature, another signal grew in with $g = 1.80$ and $A \sim 30$ G which is similar to the data found previously for the oxalate and perfluoroterephthalate single-electron oxidized species,²⁴ see Fig. 8. This matter clearly warrants further attention and is under investigation. Regrettably, the cationic complex appears kinetically labile and we have not been able to isolate the salt in a pure crystalline form.

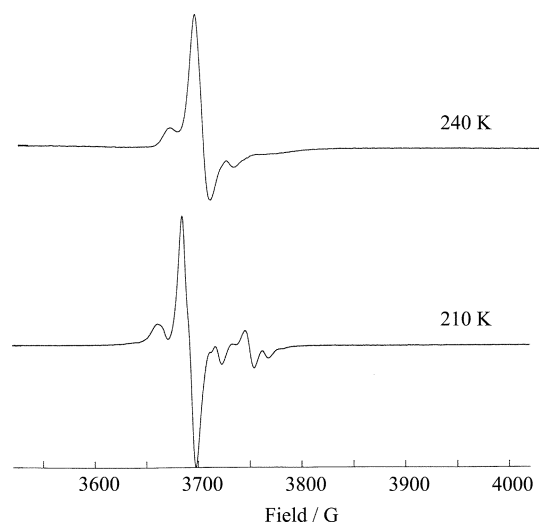


Fig. 8 X-Band EPR spectra of the radical cation [{W₂(O₂C^tBu)₃}₂(μ-9,10-An(CO₂)₂)]⁺[PF₆]⁻ in a 1 : 1 mixture of THF-CH₂Cl₂.

Concluding remarks

In this work, we have for the first time, introduced a π -conjugated dicarboxylate bridge that, by steric constraints, limits the extent of M₂ δ to bridge π to M₂ δ communication. The electronic absorption spectra are largely consistent with expectations based on the models proposed in earlier studies,^{4,5} and the electrochemical measurements also support this view. The greater delocalization that occurs for tungsten results from the closer orbital energy match and the better W 5d to bridge π overlap.

Finally, it is worth noting that the present findings support the view that the remarkable thermochromism of the perfluoroterephthalate and oxalate-bridged complexes can be traced to the Boltzmann distribution of rotamers present in solution or a glass as a function of temperature. In the present case, the thermochromism is muted by the *peri*-CH \cdots O repulsions of the 9,10-anthracene dicarboxylate bridge which impedes maximum M₂ δ -bridge- π conjugation. This work also nicely complements the recent findings of Cotton and coworkers²⁶ who studied Mo₂ quadruply-bonded centers linked by dicarboxylates of the form O₂C(CH=CH)_nCO₂ and O₂CCH=C=CHCO₂. As deduced by electrochemical measurements, these workers showed that for the conjugated series of dicarboxylates the coupling of the two M₂ centers decreased with increasing $n = 1 \rightarrow 4$ but for O₂CCH=C=CHCO₂ was essentially lost as a result of the loss of π -conjugation along the CH-C-CH chain. In the case of 9,10-anthracene dicarboxylate, the coupling is muted but not lost.

Experimental

Physical measurements

NMR spectra were recorded on a 250 MHz Bruker DPX spectrometer. All ¹H NMR chemical shifts are reported in ppm relative to the ¹H impurity in THF-d₈ at 3.58 ppm. Electronic spectra at room temperature were recorded using a Perkin-Elmer Lambda 900 spectrometer either in THF solution or in the solid-state as Nujol (Wilmad) mulls. Variable-temperature electronic spectra were obtained in the temperature range 2–100 K using an Oxford Instruments OptistatBath helium cryostat placed within the sample compartment of a Perkin-Elmer Lambda 19 UV-vis-NIR absorption spectrometer. Samples were prepared in an inert atmosphere drybox and injected into a 150 μ L copper cell consisting of two quartz windows separated by a permeable synthetic rubber spacer. Spectra of the compounds in solution were obtained in thoroughly degassed optical quality anhydrous 2-methyltetrahydrofuran (2-MeTHF, Aldrich), which forms a glass at ca. 130–140 K. All electronic spectra were taken with a scan rate of 120 nm min⁻¹, using a 1–2 nm band-pass. X-Band EPR spectra were recorded using a Bruker ESP300 Electron Spin Resonance Spectrometer. Temperature regulation was achieved using a Bruker Variable Temperature Unit. All EPR spectra were recorded in a 1 : 1 THF-CH₂Cl₂. Microanalyses were carried out by Atlantic Microlab, Inc. Cyclic voltammetric and differential voltammetric data were collected with the aid of a Princeton Applied Research (PAR) 173A potentiostat-galvanostat equipped with a PAR 176 current-to-voltage converter with *iR* compensation capability. A single-compartment voltammetric cell was equipped with a platinum working electrode, a platinum wire auxiliary electrode, and a pseudo-reference electrode consisting of a silver wire in 0.5 M ⁿBu₄NPF₆/THF separated from the bulk solution by a Vycor tip. Ferrocene was added as an

internal reference. Decamethylferrocene was used as an internal reference when the oxidation potentials of complexes were close to that of ferrocene and corrected later.

Synthesis

All reactions were carried out under an atmosphere of oxygen-free UHP-grade argon using standard Schlenk techniques or under a dry and oxygen-free nitrogen atmosphere using standard glovebox techniques. All solvents were dried and degassed by standard methods and distilled prior to use. Ditungsten tetrapivalate²⁷ and dimolybdenum tetrapivalate²⁸ were prepared by published methods. 9,10-Anthracenedicarboxylic acid, 9,10-An(CO₂H)₂, was prepared by the literature procedure⁶ and sublimed before use to remove an unknown impurity. 9,10-dibromoanthracene was purchased from Aldrich and was used as received. *n*-Butyllithium (2.5 M in hexanes) was purchased from Acros and also used as received.

[{Mo₂(O₂C^tBu)₃]₂(μ-9,10-An(CO₂)₂)]

To a flask containing 500 mg of [Mo₂(O₂C^tBu)₄] (0.839 mmol) and 20 mL of toluene was added 112 mg of 9,10-An(CO₂H)₂ (0.421 mmol). The reaction was stirred at room temperature for 8 days during which time a yellow solid precipitated from an orange solution. The yellow solid was filtered through a fine frit, and the solid washed with 3 × 10 mL of toluene and then dried under vacuum to yield 425 mg (80% yield) of the desired compound.

Microanalysis: found, C 44.00, H 5.08%. C₄₆H₆₂O₁₆Mo₄ requires C 44.03, H 4.98%. NMR (THF-d₈): δ_H (250 MHz) 1.50 (s, 18 H, O₂CC(CH₃)₃), 1.59 (s, 36H, O₂CC(CH₃)₃), 7.56 and 8.38 (both dd, 4 each, J_{HH} = 6.8 and 3.2 Hz).

[{W₂(O₂C^tBu)₃]₂(μ-9,10-An(CO₂)₂)]

To a flask containing 400 mg of [W₂(O₂C^tBu)₄] (0.518 mmol) and 20 mL of toluene was added 69 mg of 9,10-An(CO₂H)₂ (0.259 mmol). The reaction was stirred at room temperature for 7 days during which time a red solid precipitated from a blue solution. This solid was filtered through a fine frit and washed sequentially with toluene (3 × 10 mL) then hexanes (3 × 10 mL) and dried in vacuum to give 335 mg (81% yield).

Microanalysis: found, C 33.23, H 3.96%. C₄₆H₆₂O₁₆W₄ requires C 34.39, H 3.89%. NMR (THF-d₈): δ_H (250 MHz) 1.46 (s, 18 H, O₂CC(CH₃)₃), 1.52 (s, 36H, O₂CC(CH₃)₃), 7.44 and 8.25 (both dd, 4 H each, J_{HH} = 6.9 and 3.3 Hz).

[W₂(O₂C^tBu)₃]₂(μ-9,10-An(CO₂)₂)⁺PF₆⁻

In a N₂-filled drybox, a stock soln of Cp₂Fe⁺PF₆⁻ (28.5 mg) in CH₂Cl₂ (2 mL) was prepared. Of this, 1.54 mL (0.95 equiv) was added to [W₂(O₂C^tBu)₃]₂(μ-9,10-An(CO₂)₂) (107 mg, 66.6 μmol) in 2-MeTHF in a two-sided EPR apparatus. The flask was closed with Kontes tap and the resultant solution frozen in l-N₂ prior to placing in the EPR cavity. X-Band EPR spectra were recorded from 120 to 298 K. Spectra were recorded in the temperature range 180–240 K in 10 K intervals in both heating and cooling modes. Similar procedures were employed for the study of the molybdenum complex.

Molecular and electronic structure calculations

Molecular and electronic structure determinations on the models [{M₂(O₂CH)₃]₂(μ-9,10-An(CO₂)₂)] (M = Mo, W) and 9,10-anthracene dicarboxylic acid were performed with density functional theory (DFT) using the Gaussian 98¹² program, employing the B3LYP^{13–15} functional in conjunction with the 6-31G* basis set for H, C and O,¹⁶ and the SDD energy consistent pseudo-potentials for Mo and W.¹⁷ All geometries were fully optimized at the above levels using the default optimization criteria of the program. Orbital analyses were completed with GaussView.²⁹

Acknowledgements

We thank the National Science Foundation for financial support and the Ohio Supercomputer Center for computing support.

References

- 1 F. A. Cotton, C. Lin and C. A. Murillo, *Acc. Chem. Res.*, 2001, **34**, 759–771.
- 2 B. E. Bursten, M. H. Chisholm, C. M. Hadad, J. Li and P. J. Wilson, *Chem. Commun.*, 2001, 2382–2383.
- 3 B. E. Bursten, M. H. Chisholm, C. M. Hadad, J. Li and P. J. Wilson, *Isr. J. Chem.*, 2001, **41**, 187–195.
- 4 B. E. Bursten, M. H. Chisholm, R. J. H. Clark, S. Firth, C. M. Hadad, A. M. Macintosh, P. J. Wilson, P. M. Woodward and J. M. Zaleski, *J. Am. Chem. Soc.*, 2002, **124**, 3050–3063.
- 5 B. E. Bursten, M. H. Chisholm, R. J. H. Clark, S. Firth, C. M. Hadad, P. J. Wilson, P. M. Woodward and J. M. Zaleski, *J. Am. Chem. Soc.*, 2002, **124**, 12244–12254.
- 6 S. Jones, J. C. C. Atherton, M. R. J. Elsegood and W. Clegg, *Acta Crystallogr., Sect. C*, 2000, **56**, 881–883.
- 7 A. Port, M. Moragas, X. Sanchez-Ruiz, C. Jaime, A. Virgili, A. Alvarez-Larena and J. F. Piniella, *J. Org. Chem.*, 1997, **62**, 899–902.
- 8 R. L. Harlow, R. A. Loghry, H. J. Williams and S. H. Simonsen, *Acta Crystallogr., Sect. B*, 1975, **31**, 1344–1350.
- 9 C. G. Pierpont and S. A. Lang, Jr, *Acta Crystallogr., Sect. C*, 1986, **42**, 1085–1087.
- 10 M. J. Byrnes and M. H. Chisholm, *Chem. Commun.*, 2002, 2040–2041.
- 11 R. H. Cayton, M. H. Chisholm, J. C. Huffman and E. B. Lobkovsky, *J. Am. Chem. Soc.*, 1991, **113**, 8709–8724.
- 12 M. J. Frisch, G. W. Trucks, H. B. Schlegel, G. E. Scuseria, M. A. Robb, J. R. Cheeseman, V. G. Zakrzewski, J. A. J. Montgomery, R. E. Stratmann, J. C. Burant, S. Dapprich, J. M. Millam, A. D. Daniels, K. N. Kudin, M. C. Strain, O. Farkas, J. Tomasi, V. Barone, M. Cossi, R. Cammi, B. Mennucci, C. Pomelli, C. Adamo, S. Clifford, J. Ochterski, G. A. Petersson, P. Y. Ayala, Q. Cui, K. Morokuma, D. K. Malick, A. D. Rabuck, K. Raghavachari, J. B. Foresman, J. Cioslowski, J. V. Ortiz, A. G. Baboul, B. B. Stefanov, G. Liu, A. Liashenko, P. Piskorz, I. Komaromi, R. J. Gomperts, R. L. Martin, D. J. Fox, T. Keith, M. A. Al-Laham, C. Y. Peng, A. Nanayakkara, M. Challacombe, P. M. W. Gill, B. Johnson, W. Chen, M. W. Wong, J. L. Andres, C. Gonzalez, M. Head-Gordon, E. S. Replogle and J. A. Pople, Gaussian Inc., Pittsburgh, PA, 1998.
- 13 A. D. Becke, *Phys. Rev. A: Gen. Phys.*, 1988, **38**, 3098–3100.
- 14 A. D. Becke, *J. Chem. Phys.*, 1993, **98**, 5648–5652.
- 15 C. Lee, W. Yang and R. G. Parr, *Phys. Rev. B: Condens. Matter*, 1988, **37**, 785–789.
- 16 W. J. Hehre, L. Radom, P. v. R. Schleyer and J. A. Pople, *Ab initio Molecular Orbital Theory*, John Wiley & Sons: New York, 1986.
- 17 D. Andrae, U. Haeussermann, M. Dolg, H. Stoll and H. Preuss, *Theor. Chim. Acta*, 1990, **77**, 123–141.
- 18 E. K. U. Gross and W. Kohn, *Adv. Quantum Chem.*, 1990, **21**, 255–291.
- 19 R. Bauernschmitt and R. Ahlrichs, *Chem. Phys. Lett.*, 1996, **256**, 454–464.
- 20 R. E. Stratmann, G. E. Scuseria and M. J. Frisch, *J. Chem. Phys.*, 1998, **109**, 8218–8224.
- 21 S. J. A. van Gisbergen, J. G. Snijders and E. J. Baerends, *Comput. Phys. Commun.*, 1999, **118**, 119–138.
- 22 A. Rosa, E. J. Baerends, S. J. A. van Gisbergen, E. van Lenthe, J. A. Groeneveld and J. G. Snijders, *J. Am. Chem. Soc.*, 1999, **121**, 10356–10365.
- 23 F. A. Cotton and R. A. Walton, *Multiple Bonds Between Metal Atoms*, Oxford University Press, 2nd edn., 1993.
- 24 M. H. Chisholm, B. D. Pate, P. J. Wilson and J. M. Zaleski, *Chem. Commun.*, 2002, 1084–1085.
- 25 I. Noviadri, K. N. Brown, D. S. Fleming, P. T. Gulyas, P. A. Lay, A. F. Masters and L. Phillips, *J. Phys. Chem. B*, 1999, **103**, 6713–6722.
- 26 (a) F. A. Cotton, J. P. Donohue and C. A. Murillo, *J. Am. Chem. Soc.*, 2003, **125**, 5436; (b) F. A. Cotton, J. P. Donohue, C. A. Murillo and C. M. Perez, *J. Am. Chem. Soc.*, 2003, **125**, 5496.
- 27 D. J. Santure, J. C. Huffman and A. P. Sattelberger, *Inorg. Chem.*, 1985, **24**, 371–378.
- 28 A. B. Brignole and F. A. Cotton, *Inorg. Synth.*, 1971, **13**, 81–89.
- 29 Gaussian Inc., Pittsburgh, PA, 1998.
- 30 D. E. Richardson and H. Taube, *Inorg. Chem.*, 1981, **20**, 1278–1285.